ADVANCED MATERIALS
www.advmat.de

High Thermoelectric Performance in Non-Toxic Earth-Abundant Copper Sulfide

Ying He, Tristan Day, Tiansong Zhang, Huili Liu, Xun Shi, Lidong Chen,* and G. Jeffrey Snyder**

Due to the depletion of non-renewable energy resources and the deterioration of the environment caused by human energy consumption, exploitation of new types of clean energy has become more urgent. High performance thermoelectric materials and devices provide a promising possibility to easily convert energy between heat and electricity without moving parts or the release of greenhouse gases, for example in solid-state refrigeration, and power generation using industrial waste heat or automobile exhaust gas.[1–3] Industry application requires large-scale low cost, environmentally benign, and non-toxic high performance thermoelectric materials. However, current state-of-the-art thermoelectric materials are usually composed of expensive, scarce, or toxic heavy elements such as Pb, Te, Bi, Ge, Co, Sb etc.[1–3]

Thermoelectric energy conversion efficiency is generally dominated by the dimensionless thermoelectric figure of merit zT ($zT = S^2\sigma T/\kappa$),[1–3] where S is Seebeck coefficient, σ is electrical conductivity, T is absolute temperature, and κ is thermal conductivity (including electronic thermal conductivity κ_e and lattice thermal conductivity κ_L). For instance, if the efficiency of thermoelectric device is to obtain 15%, high zT values averaging at least 1.0 are needed when the temperature difference is 550 K. The value of zT in present commercial TE materials is typically less than unity. Recently, many different strategies have been effective in enhancing zT or finding new materials with high zT, such as 'phonon-glass' behavior found in caged compounds,[4] or micro-structure modification to reduce thermal conductivity,[5–8] and band structure engineering to optimize electrical properties,[9,10] as well as utilizing critical phase transition to enhance thermopower and zT.[11] In particularly, the concept of "phonon-liquid electron-crystal" (PLEC)[12] is proposed to explain the extraordinarily low thermal conductivity and high thermoelectric performance in the superionic phase of $Cu_{2-x}Se$. The advantages of liquid-like copper ions for high performance PLEC thermoelectrics include very strong phonon scattering as well as the additional reduction of specific heat due to the suppression of transverse phonon modes.[12]

The PLEC concept points out a new direction to search for novel high-performance thermoelectric materials. Superionic phases containing liquid-like ions such as $Cu_{2-x}Se$ and $Cu_{2-x}S$ thus show great potential in thermoelectrics if their electrical transport properties are similar to those of normal semiconductors. Compared to selenium, sulfur has the advantage of being low cost, environmentally benign, low toxicity, and earth-abundant (at least 10 000 times more abundant than selenium in the earth's crust). Thus thermoelectric sulfides have attracted much attention recently.[13–19] However, their zT values are so far less than other state-of-art TE materials a common problem for compounds containing non-toxic earth-abundant elements. Here, we show very low values of κ_L below 0.35 W m^{-1} K^{-1} and high values of zT about 1.7 (**Figure 1**) in non-toxic earth-abundant $Cu_{2-x}S$ with slight copper deficiency. Similar to $Cu_{2-x}Se$, liquid-like copper ions in a rigid sulfide sublattice plays the dominant role for the extraordinarily low κ_L and high zT values of $Cu_{2-x}S$.

$Cu_{2-x}S$ has been intensively studied for more than fifty years mainly focusing on its structural complexity and applications in solar cells due to its ideal band gap of 1.2 eV.[20–23] Similar to copper selenide, copper sulfide shows very complicated low temperature crystal structures. The stoichiometric compound Cu_2S possesses two phase transitions.[24] One is at about 370 K and another is around 700 K. Below 370 K it is called low chalcocite γ phase (L-chalcocite). The second is between 370 K and 700 K called high chalcocite β phase (H-chalcocite). Above 700 K, Cu_2S transfers to α phase with a *fcc* cubic structure. Similar to Cu_2Se, while the sulfur atoms maintain a rigid sublattice the Cu ions are distributed throughout many possible positions,[20] which is indicative of the high degree of disorder and low threshold for ion motion that is characteristic of liquid-like behavior. Indeed, the α phase is a classic superionic phase having freely mobile copper ions[25] while H-chalcocite β phase has recently been reported to be a solid-liquid hybrid phase with Cu in a liquid-like substructure.[26]

The high temperature thermoelectric properties of $Cu_{2-x}S$ are shown in **Figure 2**. The ideal Cu_2S without copper deficiency is an intrinsic semiconductor. Because of some copper deficiency, even in the sample with nominal composition Cu_2S, all samples show p-type conduction as holes are the dominant charge carriers. The measured room temperature carrier concentration is shown in **Table 1**. With increasing copper deficiency from Cu_2S to $Cu_{1.98}S$, and finally to $Cu_{1.97}S$, the hole concentration is significantly increased from the order of 10^{18} cm^{-3} to 10^{20} cm^{-3}, leading to the increased electrical conductivity and reduced Seebeck coefficient. The electrical conductivities are

Dr. Y. He, T. Zhang, Dr. H. Liu,
Prof. X. Shi, Prof. L. Chen
State Key Laboratory of High Performance
Ceramics and Superfine Microstructure
Chinese Academy of Sciences
1295 Dingxi Road, Shanghai 200050, China
E-mail: xshi@mail.sic.ac.cn; cld@mail.sic.ac.cn
Dr. T. Day, Prof. G. J. Snyder
Department of Materials Science
California Institute of Technology
Pasadena, California 91125, USA
E-mail: Jsnyder@caltech.edu

DOI: 10.1002/adma.201400515

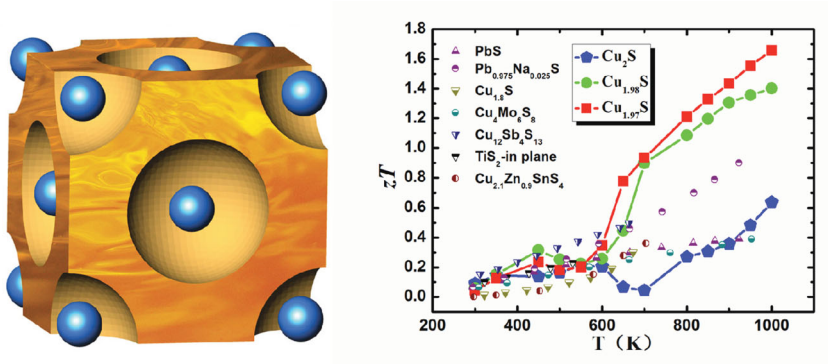

Figure 1. Thermoelectric figure of merit in non-toxic earth-abundant sulfide compounds. a, Crystal structure of cubic-chalcocite α phase of $Cu_{2-x}S$. The blue spheres represent sulfur atoms. The liquid-like copper ions travel freely within the sulfide sublattice. b, Temperature dependence of the dimensionless thermoelectric figure of merit (zT) of $Cu_{2-x}S$ and other sulfide compounds taken from refs.[12–18]

in the order of 10^4 Ω^{-1} m^{-1} and the Seebeck coefficients are ranged from 100 μV K^{-1} to 340 μV K^{-1}. Both are very suitable for good thermoelectrics, giving a power factor PF ($PF = S^2\sigma$) near 8 μW cm^{-1} K^{-2} at 1000 K as shown in Figure 2C.

The temperature dependence of the thermal conductivity is shown in Figure 2D. Compared to the electrical properties, the thermal conductivity is much less affected by copper deficiency in $Cu_{2-x}S$. In the whole experimental temperature range, the values of the total thermal conductivity of all $Cu_{2-x}S$ (x = 0, 0.02, 0.03) samples are below 0.6 W m^{-1} K^{-1}, which are remarkably low even among thermoelectric materials. Because of the low electrical conductivity, the contribution of the charge carrier thermal conductivity κ_C ($\kappa_C = L_0\sigma T$, where L_0 is the Lorenz number with the value calculated below) to the total thermal conductivity is small.

All the $Cu_{2-x}S$ samples show obviously three different behaviors in the temperature range from 300 K to 1000 K studied here. This is corresponding to the three different crystal structures mentioned above. The low-chalcocite γ phase shows an increased electrical conductivity when increasing temperature, typical of intrinsic semiconducting behavior. The cubic-chalcocite α phase shows a decreased electrical conductivity with an increase of temperature, a typical metallic behavior. Consistent with electrical conductivity, the Seebeck coefficient, power factors and thermal conductivity also show three different trends during the measured temperatures. The low temperature low-chalcocite γ phase shows a decreasing thermal conductivity when increasing temperature, typically observed in crystalline solids where acoustic phonons dominate heat transport.[27] The high temperature in high-chalcocite β and cubic-chalcocite α phases show a more temperature independent thermal conductivity (best observed without the complication of specific heat C_p in the thermal diffusivity shown in Figure S1) which indicates the high disorder of the liquid-like copper ions.

Based on the measured thermoelectric transport, the calculated thermoelectric figure of merit zT is shown in Figure 1. Similar to the individual electrical and thermal properties, the zT also shows three different trends in the measured temperature range, corresponding to the low-chalcocite γ, high-chalcocite β, and cubic-chalcocite α phases, respectively. The high band gap in $Cu_{2-x}S$ allows low electrical conductivity (Figure 2A) but enables large thermopower (Figure 2B), leading to a balanced power factor (Figure 2C). In addition, high band gap is needed for high temperature zT (Figure 1). Although the power factors of $Cu_{2-x}S$ are slightly lower than that of $Cu_{2-x}Se$, the lower thermal conductivity makes it as good if not better than $Cu_{2-x}Se$ and other traditional thermoelectric materials. Compared to other sulfides, our data obviously show at least doubled thermoelectric figure of merit at high temperatures. The measured maximum zTs reach 1.4 at 1000 K for $Cu_{1.98}S$, and 1.7 at 1000 K for $Cu_{1.97}S$, among the highest values in bulk thermoelectric materials, and greater than the highest measured zT of $Cu_{2-x}Se$, 1.5 at 1000 K.[12]

In order to understand why $Cu_{2-x}S$ appears to have superior thermoelectric performance compared to the heavier $Cu_{2-x}Se$, we modeled the electronic properties of both systems using a single parabolic band model with the electron mobility limited by acoustic phonon scattering. This model assumes a single type of carrier so we apply the model at 750 K to avoid the region of bipolar conduction in $Cu_{2-x}Se$ and to avoid the phase transition around 700 K in $Cu_{2-x}S$. Our estimates of the effective mass m^*, the mobility parameter μ_0, the deformation potential Ξ, the lattice thermal conductivity κ_L, the quality factor β, the optimum Hall carrier concentration and the maximum predicted zT of both materials are shown in **Table 2**, and the predicted curves of zT *vs.* Hall carrier concentration are shown in **Figure 3**. The Lorenz numbers calculated are about

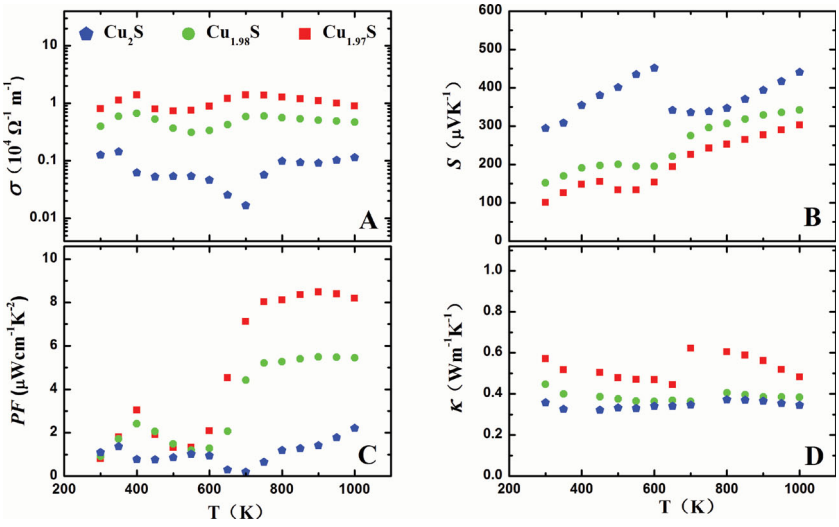

Figure 2. Temperature dependence of thermoelectric properties in $Cu_{2-x}S$. A, electrical conductivity (σ), B, Seebeck coefficient (S), C, power factor (PF), D, and thermal conductivity (κ).

Adv. Mater. **2014**,
DOI: 10.1002/adma.201400515

ADVANCED MATERIALS
www.advmat.de

Table 1. Debye temperature (θ_D), coefficients of thermal expansion (CTE) of high temperature liquid-like phases, and room temperature carrier density (p), hole mobility (μ_H), shear (v_s), longitudinal (v_l), and averaged speed of sound (v_{avg}), bulk (B_T) and shear modulus (G_T), and Grüneisen parameter (γ) of bulk materials of $Cu_{2-x}S$ (x = 0, 0.02, 0.03) and Cu_2Se.

Material	Cu_2S	$Cu_{1.98}S$	$Cu_{1.97}S$	Cu_2Se
p at 300 K [10^{19} cm^{-3}]	0.48	13.30	72.70	48.30
μ_H at 300 K [cm^2 V^{-1} s^{-1}]	16.40	1.86	0.69	15.56
p at 750 K [10^{19} cm^{-3}]	2.76	5.22	15.6	201
S at 750 K [μV K^{-1}]	338	295	242	192
v_s [m s^{-1}]	1773	1776	1763	2320
v_l [m s^{-1}]	3634	3711	3818	3350
v_{rms} [m s^{-1}]	1991	1997	1986	2523
v_{avg} [m s^{-1}]	2393	2421	2448	2663
Θ_D [K]	237	238	237	292
B_T [GPa]	50.95	54.19	59.28	27.28
G_T [GPa]	17.77	17.87	17.66	36.29
CTE [10^{-6} K^{-1}]	29.0	38.2	37.4	23.0
γ [-]	1.67	2.33	2.49	0.77
$\kappa_{min,\ all\ modes}$ [W m^{-1} K^{-1}]	0.64	0.65	0.66	0.67
$\kappa_{min,long}$ [W m^{-1} K^{-1}]	0.32	0.33	0.34	0.28
κ_u at 750 K [W m^{-1} K^{-1}]	1.6	1.1	1.0	16.9

1.6×10^{-8} V^2 K^{-2} for $Cu_{2-x}Se$ and $Cu_{2-x}S$. The quality factor, which gives an indication of thermoelectric performance at the optimum Hall carrier concentration and a temperature T, is given below.[28]

$$\beta = \frac{\mu_0 (m^*/m_e)^{3/2} T^{5/2}}{\kappa_l}. \quad (1)$$

Comparing the mobility parameters and effective masses of $Cu_{2-x}S$ and $Cu_{2-x}Se$, the numerator of the quality factor of $Cu_{2-x}Se$ is greater than that of $Cu_{2-x}S$, which explains why the highest reported power factor for $Cu_{2-x}Se$, 12 μW cm^{-1} K^{-2}, is greater than that of $Cu_{2-x}S$. However, $Cu_{2-x}S$ has a greater quality factor due to its lower lattice thermal conductivity, which is why $Cu_{2-x}S$ has a greater potential maximum zT, as shown in Figure 3. According to Figure 3 and our estimates of the optimum Hall carrier concentrations, the $Cu_{2-x}S$ samples also have Hall carrier concentrations closer to their respective optimum than do the $Cu_{2-x}Se$ samples, which is why the particular $Cu_{2-x}S$ samples measured have greater zT values than those reported for $Cu_{2-x}Se$. The detrimental effect of the higher deformation potential[28] in $Cu_{2-x}S$ is compensated by the lower effective mass[29] compared to Cu_2Se.

Table 2. Comparison of electronic band parameters and lattice thermal conductivities of $Cu_{2-x}S$ and $Cu_{2-x}Se$ at 750 K.

Material	$Cu_{2-x}S$	$Cu_{2-x}Se$
m^* [m_e]	2.1	6.5
μ_0 [cm^2 V^{-1}s^{-1}]	7.7	1.9
Ξ [eV]	5.8	2.5
κ_L [W m^{-1}K^{-1}]	0.39	0.59
β [10^4 m^3 K$^{7/2}$J^{-1}V^{-1}]	9.3	8.2
$n_{H,opt}$ [10^{20} cm^{-3}]	1.3	7.9
$(zT)_{max}$ (750K)	1	0.92

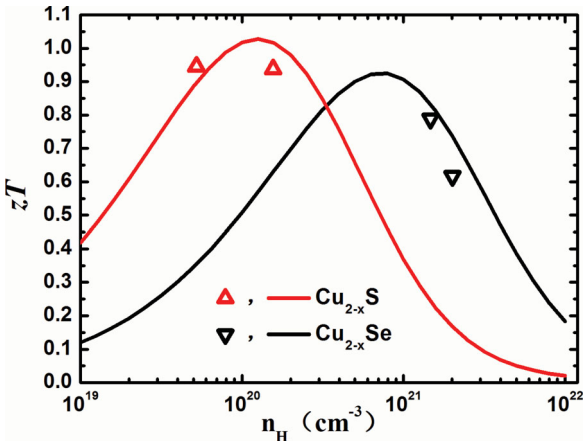

Figure 3. zT as a function of Hall carrier concentration at 750 K. Symbols are measurements and solid curves are predicted from the single parabolic band model.

The low thermal conductivity of Cu_2S is particularly surprising because Cu_2S consists of relatively light elements.[27] Small, light elements generally make stronger, more covalent bonds than the heavier elements in the same family. Such strong bonds lead to stiffer elastic constants and higher speeds of sound. This in turn leads to higher thermal conductivity in both the thermal diffusion limited regime of a disordered solid (glass) as well as the acoustic phonon dominant regime typical of crystalline solids (κ_u in Table 1). Cu_2S remarkably has lower thermal conductivity than its heavier counterpart Cu_2Se, which can be traced, in part, to its lower average speed of sound. The longitudinal speed of sound v_l (and bulk modulus, B_T) in Cu_2S is actually higher than that of Cu_2Se as one might have expected from the smaller and more covalent sulfide compared to selenide. However the transverse phonons travel much slower in Cu_2S than in Cu_2Se: the shear speed of sound v_s (and bulk modulus, G_T) are remarkably lower in Cu_2S than in Cu_2Se. This leads to an overall reduction in average speed of sound (both arithmetic and geometric averages) and lower estimate for the minimum thermal conductivity (κ_{min}) which is the expected thermal conductivity in the diffusive limit of highly disordered, amorphous solids.[30] Clearly the shear modes of Cu_2S, even in the crystalline low temperature γ phase are extraordinarily soft.

As observed in Cu_2Se the liquid-like ionic motion also leads to lower than expected heat capacity as the modes can no longer store elastic energy. This reduction in heat capacity is even more pronounced in Cu_2S than in Cu_2Se, as shown in **Figure 4**. While Cu_2Se shows an essentially temperature independent C_p up to 800K, the C_p of Cu_2S is clearly decreasing to below the Dulong-Petit value derived for solids with shear modes that store elastic energy. The reduced C_p in β phase is consistent with the report by Gronvold and Westrum.[31] The low and decreasing C_V leads to low thermal conductivity due to its contribution to $\kappa_L \sim v_{avg} C_V l/3$ (l is phonon mean free path),

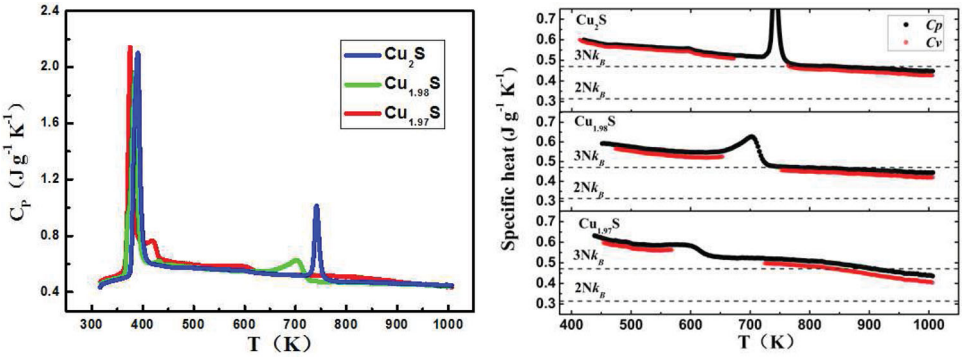

Figure 4. Temperature dependence of the heat capacity of $Cu_{2-x}S$ (x = 0, 0.02, 0.03) at constant pressure (C_p) and volume (C_V). The enlarged view of the curves between 450 K and 1000 K is shown in the right picture.

but this may also be an indicator of extreme softening of shear modes that drastically reduces the transverse phonon velocity.

The special character of PLEC makes copper sulfide possess a very low lattice thermal conductivity in ways not previously recognized in Cu_2Se. The findings in Cu_2S also suggest that Liquid-like materials may also possess inherently low speed of sound and high Grüneisen parameter (which also contributes to greater umklapp scattering and therefore lower κ_u).

The estimated lattice thermal conductivity from measurements of Cu_2S is below even that expected for a glass or even normal liquid. The minimum thermal conductivity κ_{min} calculated from the high temperature limit of Cahill's formula[30] in Table 1,

$$\kappa_{\min} = \frac{1}{2}\left(\frac{\pi}{6}\right)^{1/3} kV^{-2/3}(2v_t + v_l) \quad (2)$$

should give a good estimate for the lattice thermal conductivity when all of the phonons (transverse and longitudinal) completely scattered. This is typically a good estimate not only for solid amorphous glasses but also liquids whose thermal conductivity does not differ significantly from that of glasses.[32] Some low dimensional structures, however, do show thermal conductivity significantly below κ_{min} that appears to be due to the reduction of number of heat propagating modes, particularly shear modes.[33] If some shear modes (approximately half) are removed from the formula of κ_{min} from Cahill, values close to these measured for $Cu_{2-x}S$ and Cu_2Se are calculated. If only the longitudinal modes contribute, $\kappa_{min,long}$ is calculated (Table 1). Thus the reduction in heat capacity of the shear modes appear to reduce the lattice thermal conductivity to below that of a normal amorphous solid.

In conclusion, we show that liquid-like copper sulfide $Cu_{2-x}S$ has exceptional thermal and electrical transport properties and extends the concept of PLEC thermoelectric materials. The electrical transport can be modeled as a heavily doped semiconductor where Cu_2S lower effective mass than Cu_2Se, which leads to higher mobility but the higher deformation potential counteracts any gains in quality factor. The disordered copper ions in the solid or liquid-like sublattice not only strongly scatter lattice phonons they also diminish the heat capacity of lattice vibrations much more clearly in Cu_2S than in Cu_2Se. This stronger PLEC effect in Cu_2S than observed in Cu_2Se also is correlated to the extraordinarily low transverse acoustic phonon velocity as well as anharmonicity as measured by Grüneisen parameter, both of which further leads to low thermal conductivity. As a result, the total thermal conductivity in $Cu_{2-x}S$ is less than 0.6 W m^{-1} K^{-1} in the whole temperature range, leading to a maximum zT value of 1.7 at 1000 K. We expect the discovery of high thermoelectric performance copper sulfides could attract great attention within the waste heat recovery industry due to their unique combination of elements that are low cost, non-toxic, and earth-abundant.

Experimental Section

$Cu_{2-x}S$ samples were prepared by directly melting the elements Cu (shots, 99.999%, Alfa Aesar) and S (pieces, 99.999%, Alfa Aesar) in sealed silica tubes under vacuum. The element mixtures (the reported compositions are nominal compositions) were heated at a speed of 4 K min^{-1} to 1383 K and then remain at this temperature for 18 hours to ensure complete melting of all elements before quenching into ice water. Next, the ingots were ground into fine powders, and then pressed into pellets for annealing at 833 K for 7 days. Finally, the obtained pellets were crushed into powders and consolidated by spark plasma sintering (Sumitomo SPS-2040) at 713 K under a pressure of 65 MPa for 5 minutes. The powder samples before spark plasma sintering were characterized by X-ray diffraction with Cu Kα radiation at room temperature. The high-temperature Seebeck coefficient and electrical resistivity were measured using Ulvac ZEM-3. The thermal diffusivity (D) data were obtained by laser flash method using Netzsch LFA457, and the specific heat (C_p) was measured by differential scanning calorimetric using Netzsch DSC 404F3. The mass of all the samples is unchanged after DSC measurements. The density (d) was measured using the Archimedes method. The thermal conductivity was calculated from $\kappa = D \times C_p \times d$. The Hall resistance ($R_H$) was measured using a Quantum Design PPMS and a custom built system.[34] The hole mobility (μ_H) and carrier concentration (p) were calculated from $p = 1/eR_H$ and $\mu_H = \sigma/pe$, where σ is the electrical conductivity by and e is the elementary charge. The thermal expansion coefficient is measured by a Netzsch DIL 402C. The sound speed was measured using ultrasound pulses.

Supporting Information

Supporting Information is available from the Wiley Online Library or from the author.

Adv. Mater. 2014,
DOI: 10.1002/adma.201400515

Acknowledgements

This work is supported by National Basic Research Program of China (973-program) under Project No. 2013CB632501, National Natural Science Foundation of China (NSFC) under the No. 51222209 and 51121064, and AFOSR MURI.

Received: January 31, 2014
Published online:

[1] L. E. Bell, *Science* **2008**, *321*, 1457 .
[2] G. J. Snyder, E. S. Toberer, *Nat. Mater.* **2008**, *7*, 105.
[3] A. F. Ioffe, Infosearch Limited, London, **1957**.
[4] B. C. Sales, D. Mandrus, R. K. Williams, *Science* **1996**, *272*, 1325.
[5] K. F. Hsu, S. Loo, F. Guo, W. Chen, J. S. Dyck, C. Uher, T. Hogan, E. K. Polychroniadis, M. G. Kanatzidis, *Science* **2004**, *303*, 818.
[6] A. I. Hochbaum, R. K. Chen, R. D. Delgado, W. J. Liang, E. C. Garnett, M. Najarian, A. Majumdar, P. D. Yang, *Nature* **2008**, *451*, 163.
[7] K. Biswas, J. Q. He, I. D. Blum, C. I. Wu, T. P. Hogan, D. N. Seidman, V. P. Dravid, M. G. Kanatzidis, *Nature* **2012**, *489*, 414.
[8] L. D. Hicks, M. S. Dresselhaus, *Phys .Rev. B* **1993**, *47*, 12727.
[9] Y. Z. Pei, X. Shi, A. LaLonde, H. Wang, L. D. Chen, G. J. Snyder, *Nature* **2011**, *473*, 66.
[10] J. P. Heremans, V. Jovovic, E. S. Toberer, A. Saramat, K. Kurosaki, A. Charoenphakdee, S. Yamanaka, G. J. Snyder, *Science* **2008**, *321*, 554.
[11] H. L. Liu, X. Yuan, P. Lu, X. Shi, F. F. Xu, Y. He, Y. S. Tang, S. Q. Bai, W. Q. Zhang, L. D. Chen, Y. Lin, L. Shi, H. Lin, X. Y. Gao, X. M. Zhang, H. Chi, C. Uher, *Adv. Mater.* **2013**, *25*, 6607.
[12] H. L. Liu, X. Shi, F. F. Xu, L. L Zhang, W. Q. Zhang, L. D. Chen, Q. Li, C. Uher, D. Tristan, G. J. Snyder, *Nat. Mater.* **2012**, *11*, 422.
[13] Z. H. Ge, B. P. Zhang, Y. X. Chen, Z. X. Yu, Y. Liu, J. F. Li, *Chem. Commun.* **2011**, *47*, 12697.
[14] C. Wan, Y. F. Wang, N. Wang, W. Norimatsu, M. Kusunoki, K. Koumoto, *Sci. Technol. Adv. Mater.* **2010**, *11*, 044306.
[15] L. D. Zhao, J. He, S. Hao, C. L. Wu, T. P. Hogan, C. Wolverton, V. P. Dravid, M. G. Kanatzidis, *J. Am. Chem. Soc.* **2012**, *134*, 16327.
[16] K. Suekuni, K. Tsuruta, M. Kunii, H. Nishiate, E. Nishibori, S. Maki, M. Ohta, A. Yamamoto, M. Koyano, *J. Appl. Phys.* **2013**, *113*, 043712.
[17] M. Ohta, H. Obara, A. Yamamoto, *Mater. Trans.* **2009**, *50*, 2129.
[18] M. L. Liu, F. Q. Huang, L. D. Chen, W. Chen, *Appl. Phys. Lett.* **2009**, *94*, 202103.
[19] X. Lu, D. T. Morelli, Y. Xia, F. Zhou, V. Ozolins, H. Chi, X. Y. Zhou, C. Uher, *Adv. Energy Mater.* **2013**, *3*, 342.
[20] Q. Xu, *Appl. Phys. Lett.* **2012**, *100*, 061906.
[21] H. T. Evans, *Nature* **1971**, *232*, 69.
[22] G. P. Sorokin, Y. M. Papshev, P. T. Oush, *Sov. Phys. Solid State* **1966**, *7*, 1810.
[23] S. Kashida, W. Shimosaka, M. Mori, D. Yoshimura, *J. Phys. Chem. Solids* **2003**, *64*, 2357.
[24] D. J. Chakrabarti, D. E. Laughlin, *Bull. Alloy Phase Diagrams* **1983**, *4*, 254.
[25] E. Hirahara, *J. Phys. Soc. Jpn.* **1951**, *6*, 422.
[26] L. W. Wang, *Phys. Rev. Lett.* **2012**, *108*, 085703.
[27] E. S. Toberer, A. Zevalkink, G. J. Snyder, *J. Mater. Chem.* **2011**, *21*, 15843.
[28] H. Wang, Y. Z. Pei, A. D. LaLonde, G. J. Snyder, *Proc. Natl. Acad. Sci. USA* **2012**, *109*, 9705.
[29] Y. Z. Pei, H. Wang, G. J. Snyder, *Adv. Mater.* **2012**, *24*, 6125.
[30] D. G. Cahill, S. K. Watson, R. O. Pohl, *Phys. Rev. B* **1992**, *46*, 6131.
[31] F. Gronvold, E. F. Westrum, *J. Chem. Thermodynamics* **1987**, *19*, 1183.
[32] G. A. Slack, *Solid State Phys.* **1979**, *34*, 1.
[33] C. Chiritescu, G. C. David, N. Ngoc, J. David, B. Arun, K. Pawel, Z. Paul, *Science* **2007**, *315*, 351.
[34] K. A. Borup, E. S. Toberer, L. D. Zoltan, G. Nakatsukasa, M. Errico, J. P. Fleurial, B. B. Iverson, G. J. Snyder, *Rev. Sci. Instrum.* **2012**, *83*, 123902.